JACS
JOURNAL OF THE AMERICAN CHEMICAL SOCIETY
Article
pubs.acs.org/JACS

Synthesis, Electrochemistry, and Photophysics of a Family of Phlorin Macrocycles That Display Cooperative Fluoride Binding

Allen J. Pistner,[†] Daniel A. Lutterman,[‡] Michael J. Ghidiu,[†] Ying-Zhong Ma,[‡] and Joel Rosenthal*,[†]

[†]Department of Chemistry and Biochemistry, University of Delaware, Newark, Delaware 19716, United States
[‡]Chemical Sciences Division, Oak Ridge National Laboratory, Oak Ridge, Tennessee 37831, United States

Supporting Information

ABSTRACT: A homologous set of 5,5-dimethylphlorin macrocycles in which the identity of one aryl ring is systematically varied has been prepared. These derivatives contain ancillary pentafluorophenyl (3H(Phl^{F})), mesityl (3H(Phl^{Mes})), 2,6-bismethoxyphenyl (3H(Phl^{OMe})), 4-nitrophenyl (3H(Phl^{NO_2})), or 4-*tert*-butylcarboxyphenyl (3H(Phl^{CO_2tBu})) groups at the 15-*meso*-position. These porphyrinoids were prepared in good yields (35−50%) and display unusual multielectron redox and photochemical properties. Each phlorin can be oxidized up to three times at modest potentials and can be reduced twice. The electron-donating and electron-releasing properties of the ancillary aryl substituent attenuate the potentials of these redox events; phlorins containing electron-donating aryl groups are easier to oxidize and harder to reduce, while the opposite trend is observed for phlorins containing electron-withdrawing functionalities. Phlorin substitution also has a pronounced effect on the observed photophysics, as introduction of electron-releasing aryl groups on the periphery of the macrocycle is manifest in larger emission quantum yields and longer fluorescence lifetimes. Each phlorin displays an intriguing supramolecular chemistry and can bind 2 equiv of fluoride. This binding is allosteric in nature, and the strength of halide binding correlates with the ability of the phlorin to stabilize the buildup of charge. Moreover, fluoride binding to generate complexes of the form 3H(Phl^{R})·2F^{-} modulates the redox potentials of the parent phlorin. As such, titration of phlorin with a source of fluoride represents a facile method to tune the ability of this class of porphyrinoid to absorb light and engage in redox chemistry.

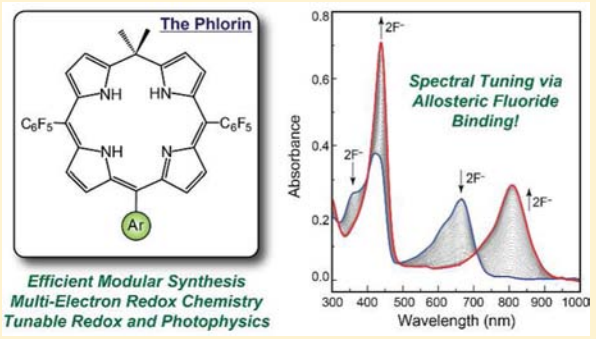

INTRODUCTION

Porphyrin is a ubiquitous and versatile protein cofactor that plays many roles in biology.[1] The heme cofactor, which is the iron complex of protoporphyrin IX, is the most common form of porphyrin found in nature. By control of the axial coordination of the iron atom, as well as hydrogen-bonding and other noncovalent interactions with the porphyrin periphery, protein environments successfully tune the electronic/redox properties of the cofactor.[2] This electronic tailoring allows enzymatic systems to effect a wide range of redox processes such as single-electron transfer by cytochromes,[3] dioxygen coordination and transport by globins,[4] O−O bond activation and substrate oxidation by cytochrome P-450,[5] and peroxide/superoxide removal by peroxidases and catalases.[6]

In addition to making use of tetrapyrroles as platforms for important catalytic transformations, nature also relies on porphyrin-based chromophores for solar light harvesting. Plants[7,8] and cyanobacteria[9] both make use of chlorophylls and other natural porphyrinoids to absorb sunlight in the UV−vis region. These biological systems have driven the widespread study of photoinduced electron transfer by synthetic porphyrin constructs[10,11] and inspired the use of porphyrin chromophores in DSC assemblies.[12,13] Traditionally, such systems have displayed light conversion efficiencies below 7%.[14,15] These low efficiencies are partly due to the fact that simple porphyrin derivatives display relatively narrow absorbances in the Soret (375−425 nm) and Q-band (500−600 nm) regions, which limits light capture at longer wavelengths (650−900 nm). Nature confronts this issue by using carotenoids to harvest photons on the low energy end of the visible region.[16−18] Furthermore, recent work has shown that designer porphyrins incorporating ancillary electron donors and extended π-conjugation display much broader absorption profiles upon incorporation into DSC devices, giving rise to solar conversion efficiencies in excess of 12%.[19]

Despite their ubiquitous role in biology and chemistry, porphyrins only represent a subset of tetrapyrrole macrocycles that display rich photophysical properties. Phthalocyanines and corroles are two non-natural porphyrinoids that have been used for light harvesting applications. Additional tetrapyrrole macrocycles include porphyrinogens and other porphyrin derivatives with sp^3 hybridized *meso*-carbons.[20−23] Unlike conventional porphyrinoids, these compounds display an intriguing multielectron redox chemistry due to the sp^3 hybridized *meso*-

Received: February 10, 2013
Published: April 17, 2013

dx.doi.org/10.1021/ja401391z | J. Am. Chem. Soc. 2013, 135, 6601−6607

carbons; however, the lack of π-conjugation between pyrrole units compromises the spectroscopic properties of these macrocycles in comparison to the rich photophysics typical of porphyrins.[24]

We recently detailed the phlorin macrocycle, in which a single sp^3 hybridized carbon is introduced at one of the *meso*-positions.[25] This structure engenders multielectron redox properties and intriguing photophysical characteristics, which distinguish it from more common tetrapyrrole architectures such as porphyrins and corroles (Chart 1).[25] To this point,

Chart 1

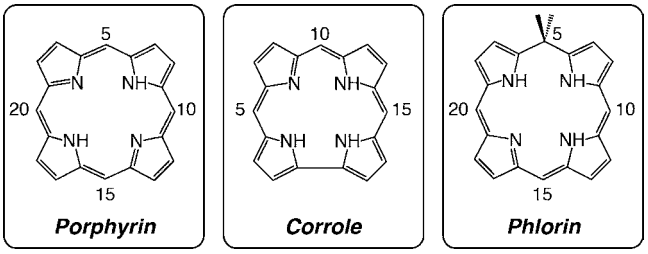

however, only a handful of 5,5-dimethylphlorins have appeared in the literature[25−27] and the general redox and photophysical properties of such systems remain largely unknown. In order to gain a better appreciation for the manner in which synthetic alterations attenuate the electronic structure of the phlorin construct, we have undertaken the preparation and physical characterization of a family of phlorin homologues. This work demonstrates that the multielectron redox and photochemical properties are inherent to the phlorin core and that these properties can be tuned by variation of the ancillary aryl groups appended to the phlorin framework. We have also uncovered that these macrocycles display an unusual supramolecular chemistry with fluoride anions and that cooperative binding of fluoride to the phlorin core significantly perturbs the electronic structure of the chromophore as judged by UV−vis absorption and electrochemistry measurements.

RESULTS AND DISCUSSION

The family of phlorin derivatives under consideration was prepared by adapting a modular synthetic methodology (Scheme 1).[25,28] This route begins with the preparation of a diacylated dipyrromethane (**1**) via the deprotonation of 5,5-dimethyldipyrromethane with EtMgBr, followed by addition of pentafluorophenylbenzoyl chloride. Reduction of **1** with $NaBH_4$ in THF/MeOH (3:1) generated the corresponding dicarbinol, which was condensed with various 5-aryldipyrromethane derivatives (**2**−**6**)[29,30] in the presence of TFA to yield the corresponding phlorin frameworks, following oxidation with DDQ and purification by flash chromatography. The modular nature of this synthetic method provided phlorin derivatives with an ancillary pentafluorophenyl (3H(Phl^F)), mesityl (3H(Phl^{Mes})), 2,6-bismethoxyphenyl (3H(Phl^{OMe})), 4-nitrophenyl (3H(Phl^{NO_2})), or 4-*tert*-butylcarboxyphenyl (3H-(Phl^{CO_2tBu})) substituent at the *meso*-position across from the sp^3 hybridized center of the phlorin core in 35−50% yield. These yields are relatively high compared to those of typical porphyrin syntheses and scale up well to roughly 0.5 g. We note that synthesis of the family of porphyrinoids shown in Scheme 1 nearly triples the library of known 5,5-dimethylphlorin derivatives that have been reported to date.

With each of the phlorins of Scheme 1 in hand, we sought to characterize the photophysical and redox properties of these compounds. Solutions of each of these macrocycles are an intense emerald green color and display broadly absorbing bands across the visible region from 300 to 750 nm (Figure 1). Variation of the substituents on the aryl group at the 15-position of the phlorin ring does not drastically attenuate the shape of the corresponding absorption profiles. Subtle changes in the extinction coefficients for both the Soret and Q-band regions are observed, with the more electron rich phlorins (i.e., 3H(Phl^{Mes}) and 3H(Phl^{OMe})) displaying more strongly absorbing bands compared to 3H(Phl^F).

Similar trends are observed for the emission profiles for each of the phlorins studied. Each of the porphyrinoids produces a broad emission profile upon excitation into the Q-band region,

Scheme 1. Synthesis of a Family of Phlorins with Varying Substitutents at the 15-*meso*-Position

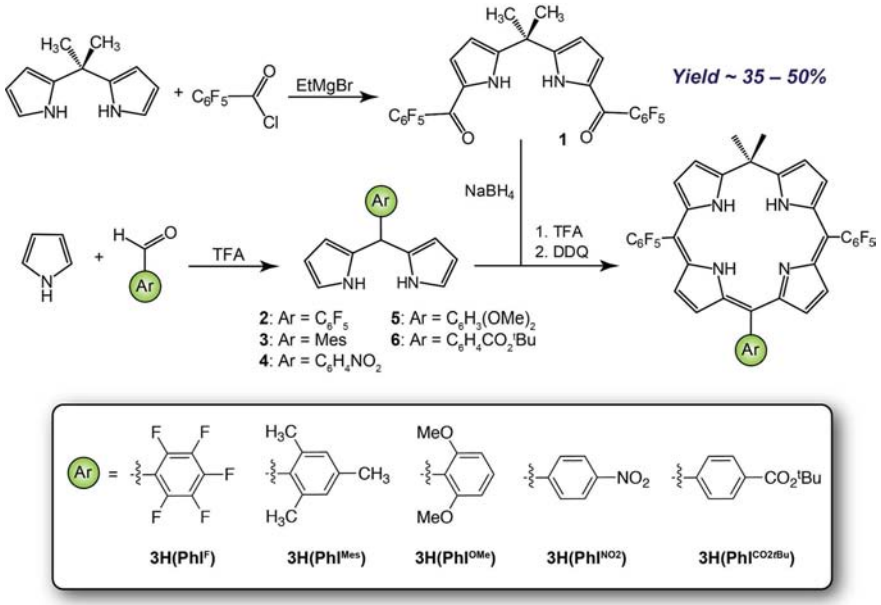

dx.doi.org/10.1021/ja401391z | J. Am. Chem. Soc. 2013, 135, 6601−6607

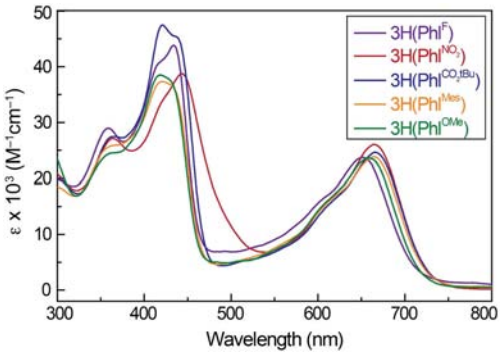

Figure 1. UV−vis absorption spectra recorded for each of the phlorins studied in CH_2Cl_2.

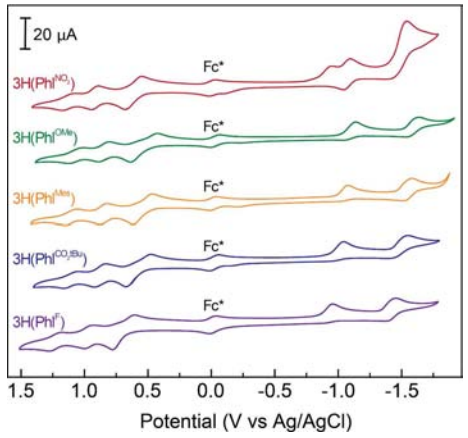

Figure 2. Cyclic voltammograms recorded for a family of 5,5-dimethylphlorin derivatives (1.0 mM) at a scan rate of 50 mV/s in CH_2Cl_2 containing $TBAPF_6$ with an internal decamethylferrocene standard (FC*).

with fluorescence maxima centered between 720 and 732 nm (Figure S1 in Supporting Information). Table 1 highlights the photoluminescence data obtained for these compounds, including the quantum yields (Φ_{Fl}) of emission, which range from 5.3×10^{-4} for the most electron deficient phlorin (3H(Phl^{F})) to 17.6×10^{-4} for the methoxy substituted macrocycle (3HPhl^{OMe}). In keeping with these low fluorescence quantum yields, the emission lifetimes (τ_{Fl}) observed for each of these systems are short compared to those of typical freebase porphyrin derivatives;[31−33] the phlorin lifetimes range from ∼37 ps for 3H(Phl^{F}) to ∼101 ps for 3H(Phl^{OMe}). The nitro (3H(Phl^{NO_2})), mesityl (3H(Phl^{Mes})), and *tert*-butyl ester (3H(Phl^{CO_2tBu})) phlorin derivatives display fluorescence lifetimes of 37, 58, and 66 ps, respectively. These represent the first measurements of excited state lifetimes of 5,5-dimethylphlorin frameworks. As shown in Table 1, the observed trend in τ_{Fl} values for each of the phlorins parallels that observed for Φ_{Fl}, with more electron rich phlorin constructs displaying longer-lived excited states and larger emission quantum yields.

Each of the phlorin architectures of Scheme 1 also displays redox properties that are attenuated by the aryl substituent at the 15-*meso*-position. Cyclic voltammetry experiments were carried out for 1.0 mM solutions of each of these porphyrinoids in CH_2Cl_2 containing 0.1 M $TBAPF_6$ and an internal decamethylferrocene standard. The resulting CV traces are reproduced in Figure 2. Each phlorin displays reduction waves at roughly −1.0 and −1.5 V versus Ag/AgCl. Both these redox events are largely irreversible. This is especially apparent for the first reduction, for which cathodic and anodic peak potentials are separated by approximately 0.8 V for each of the phlorins other than 3H(Phl^{F}). Furthermore, these reduction potentials are perturbed by incorporation of electron releasing groups on the aryl ring at the 15-*meso*-position. DPV experiments (Figure S2) reveal that the reduction potentials for the phlorins studied in this work increase to more negative potentials along the series 3H(Phl^{F}) ($E_{1/2}$ = −0.93 V) ∼ 3H(Phl^{NO_2}) ($E_{1/2}$ = −0.94 V) < 3H(Phl^{CO_2tBu}) ($E_{1/2}$ = −0.99 V) < 3H(Phl^{Mes}) ($E_{1/2}$ = −1.05 V) ∼ 3H(Phl^{OMe}) ($E_{1/2}$ = −1.07 V) versus Ag/AgCl. The reduction waves for the nitro-substituted phlorin (3H(Phl^{NO_2})) are significantly attenuated compared to the other phlorins studied. This difference is likely due to redox events involving reduction of the nitro functionality, as has been observed for analogous porphyrin derivatives.[34]

Each of the phlorin macrocycles also displays three quasi-reversible oxidations between 0.6 and 1.25 V. These redox potentials are also influenced by the electronic nature of the aryl substituent at the phlorin 15-*meso*-position, as summarized in Table 1. Inclusion of electron donating groups shifts each of the three oxidations to significantly less positive potentials compared to those observed for 3H(Phl^{F}). For example, both 3H(Phl^{OMe}) and 3H(Phl^{Mes}) display similar potentials for each of the oxidation events, which occur at approximately 0.6, 0.9, and 1.1 V versus Ag/AgCl. The first oxidation potentials observed for these porphyrinoids are especially low and are close to that of ferrocene,[35] which is a quintessential organometallic electron donor. Moreover, the first oxidation potentials of these species are nearly a full volt lower than those observed for analogous fluorinated porphyrin derivatives,[25,36] which further highlights the distinctive electronic nature of the

Table 1. Redox and Photophysical Data Recorded for Homologous Phlorin Derivatives

	redox properties[a]						absorption[b]		emission[b]		
	$E_{ox}(1)$, V	$E_{ox}(2)$, V	$E_{ox}(3)$, V	$E_{red}(1)$, V	$E_{red}(2)$, V	E_{0-0}, V	Soret λ_{max}, nm (ε, cm^{-1} M^{-1})	Q band λ_{max}, nm (ε, cm^{-1} M^{-1})	λ_{em}, nm	τ_{Fl}, ps	Φ_{Fl}
3H(Phl^{F})	0.75	0.99	1.26	−0.93	−1.43	1.68	435 (29300)	655 (16000)	722	37	5.34×10^{-4}
3H(Phl^{NO_2})	0.65	0.93	1.16	−0.94	−1.53	1.73	445 (30800)	670 (21200)	732	37	6.35×10^{-4}
3H(Phl^{CO_2tBu})	0.63	0.89	1.12	−0.99	−1.49	1.62	435 (45100)	665 (24700)	731	66	9.96×10^{-4}
3H(Phl^{Mes})	0.60	0.87	1.14	−1.05	−1.56	1.65	420 (36400)	669 (24200)	721	58	9.65×10^{-4}
3H(Phl^{OMe})	0.61	0.87	1.10	−1.07	−1.58	1.68	415 (38400)	665 (24900)	720	101	17.6×10^{-4}

[a]Redox potentials are referenced to Ag/AgCl. [b]All spectroscopic data were recorded for phlorin samples in deoxygenated CH_2Cl_2 solution. Fluorescence data were recorded by exciting solutions of each of the phlorins at λ = 650 nm. Time-resolved fluorescence data were recorded by exciting the solution samples of each of the phlorins at λ = 650 nm and monitoring the emission at λ = 750 nm. The lifetime of the dominant decay component with relative amplitude >97% is shown for each phlorin derivative.

dx.doi.org/10.1021/ja401391z | J. Am. Chem. Soc. 2013, 135, 6601−6607

phlorin framework. The electron-withdrawing aryl groups of 3H(Phl^{CO_2tBu}) and 3H(Phl^{NO_2}) increase the observed potentials of the oxidation waves by 10−15 mV to values between those of the most electron deficient (3H(Phl^{F})) and rich (3H(Phl^{OMe})) architectures (Table 1).

The relatively low first oxidation potentials observed for each member of the phlorin family of Scheme 1 give rise to compressed electrochemical HOMO−LUMO gaps compared to typical fluorinated porphyrins.[25] This contraction is consistent with the significant absorption bands displayed by the phlorins at energies lower than 600 nm (vide supra). As displayed in Table 1, HOMO−LUMO gaps (E_{0-0}) for most of the phlorins range from 1.65 to 1.75 eV; however, 3H(Phl^{CO_2tBu}) has a notably small HOMO−LUMO gap of ∼1.62 eV and is the smallest of all the phlorin constructs we have studied to date. Each of these E_{0-0} values is significantly lower than those observed for typical fluorinated porphyrin (∼2.4 V) and corrole frameworks (∼1.85 V).[25]

The phlorin supports a notable supramolecular chemistry via formation of hydrogen bonds between the pyrrole N−H units and fluoride anions. Similar chemistry has been documented for calipyrroles[37−39] and other polypyrrolic platforms.[40−43] Slow titration of anhydrous CH_2Cl_2 solutions (10 μM) of each of the systems shown in Scheme 1 with *n*-tetrabutylammonium fluoride (TBAF) results in a change in color from emerald green to light brown. This colorimetric transformation can be closely monitored by UV−vis spectroscopy. Indeed, slow addition of TBAF aliquots is manifest in shifts in both the visible and near-IR regions of the phlorin absorption spectrum. As shown in Figure 3, fluoride binding to 3H(Phl^{Mes}) is

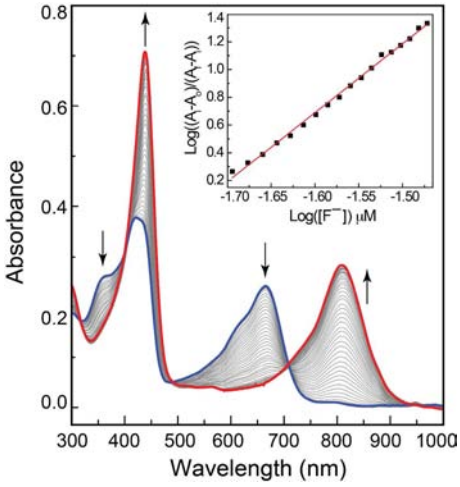

Figure 3. Changes in the UV−vis absorption profile of 3H(Phl^{Mes}) upon titration with TBAF. Inset: Hill plot confirming the allosteric formation of 3H(Phl^{Mes})·2F$^-$.

accompanied by a large increase in absorptivity in the Soret region at ∼420 nm, as well as a dramatic shift of the Q-band region from ∼670 to 805 nm. Although TBAF can be basic, ^{1}H and ^{19}F NMR studies conducted for 3H(Phl^{F}) confirm that the observed UV−vis spectral changes are consisitent with hydrogen-bonding of fluoride to the phlorin N−H groups and not deprotonation of the macrocycle.[25] UV−vis titration data for each of the phlorins of Scheme 1 are qualitatively similar to data presented for 3H(Phl^{Mes}) and are reproduced in the Supporting Information (Figure S3).

For each titration, well-anchored isosbestic points are maintained during the course of the fluoride binding experiment, which would suggest a clean conversion of freebase phlorin (3H(Phl^{R})) to a 1:1 fluoride adduct, without the formation of any intermediary species. Job analysis of the fluoride binding for each of the phlorins indicates that binding is not 1:1, however. Each Job plot (Figure S4) maximizes at a phlorin molar ratio of ∼0.3 to 0.35, indicating that the phlorins are capable of binding 2 equiv of fluoride to generate 3H(Phl^{R})·2F$^-$. Although this binding stoichiometry is uncommon for simple tetrapyrrole platforms, such behavior has been observed for a phlorin construct containing a dangling pyrrole moiety at the sp^3 center[44] and for 3H(Phl^{F}) in THF.[25] We note that unlike other protonated porphyrinoids that can bind larger halogens such as chloride,[45,46] none of the phlorins of Scheme 1 bind halogens other than fluoride, as judged by UV−vis spectroscopy.

A Hill analysis of the titration data for 3H(Phl^{Mes}) (Figure 3, inset) supports the 2:1 binding model. This analysis produces a well-fit linear regression and yields a cooperativity constant of $\beta_2 = 4.5 \times 10^8$ M^{-2} for formation of ternary complex 3H(Phl^{Mes})·2F$^-$. The magnitude of this β_2 value attests to the strength of the fluoride binding interaction. Similar to previous studies in THF,[25] Hill analysis of fluoride binding to 3H(Phl^{Mes}) does not allow for the individual equilibrium constants (K_1 and K_2) for formation of 3H(Phl^{Mes})·F$^-$ and 3H(Phl^{Mes})·2F$^-$ to be extracted from the titration data but reveals the extent to which allosteric effects drive fluoride binding. It is clear, however, that the equilibrium constant for binding of the second fluoride ion (K_2) to generate 3H(Phl^{Mes})·2F$^-$ is much larger than that for the first binding event (K_1) and suggests that a destabilizing conformational change to the phlorin core may occur upon binding of the first fluoride to produce 3H(Phl^{R})·F$^-$. The cooperative nature of fluoride binding precludes the build-up of a singly fluoride bound species in solution and gives rise to the isosbestic crossings observed for the UV−vis titration. The fact that there is no observable singly fluoride bound intermediate (3H(Phl^{Mes})·F$^-$) is consistent with this binding model.

$$3H(Phl^R) + F^- \rightleftarrows 3H(Phl^R)\cdot F^- \quad (1)$$

$$3H(Phl^R)\cdot F^- + F^- \rightleftarrows 3H(Phl^R)\cdot 2F^- \quad (2)$$

Hill analyses for the fluoride titrations recorded for each of the other four phlorins (Figure S3) have also been carried out. The resulting Hill plots are reproduced in Figure S5, and the corresponding binding parameters are presented in Table 2. Each of the systems studied displays β_2 values that are greater than 10^8 M^{-2}, establishing that each of the phlorins is capable of strongly coordinating 2 equiv of fluoride to generate 3H(Phl^{R})·2F$^-$. There exists a general trend that shows that cooperative fluoride binding is strongest for the more electron

Table 2. Thermodynamic Parameters for Binding of Fluoride to Freebase Phlorins

	β_2, M^{-2}	Hill constant (η)	$\Delta E_{ox}(1)$, mV	$\Delta E_{red}(1)$, mV
3H(Phl^{F})	1.6×10^{15}	8.6	210	450
3H(Phl^{NO_2})	2.5×10^{12}	7.4	540	420
3H(Phl^{CO_2tBu})	2.4×10^{10}	5.1	470	320
3H(Phl^{Mes})	4.5×10^{8}	5.0	400	280
3H(Phl^{OMe})	6.3×10^{9}	5.4	410	260

dx.doi.org/10.1021/ja401391z | J. Am. Chem. Soc. 2013, 135, 6601−6607

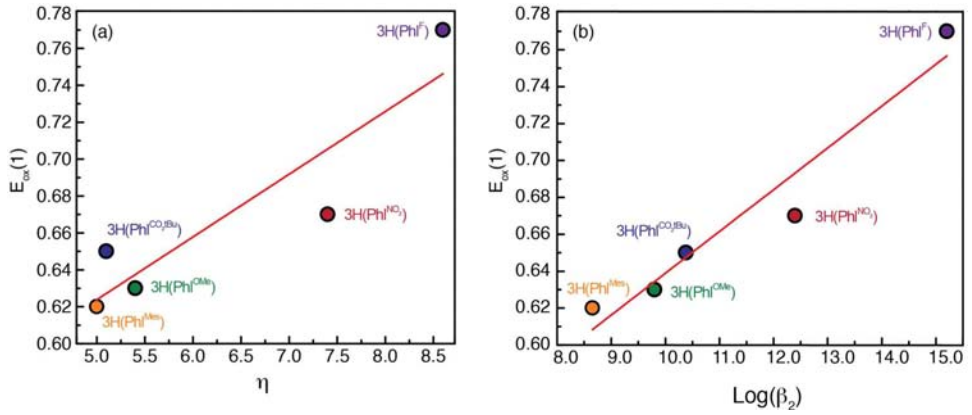

Figure 4. Correlation between phlorin oxidation potential and (a) Hill coefficient (η) and (b) strength of fluoride binding (β_2).

deficient phlorin frameworks, including 3H(Phl^{F}) and 3H(Phl^{NO_2}). By contrast, the phlorin macrocycles containing electron-releasing groups at the 15-*meso*-position such as 3H(Phl^{Mes}) and 3H(Phl^{OMe}) are weaker fluoride binders. This trend can be rationalized in a general sense, as a hard fluoride anion is expected to be more strongly attracted to hydrogen-bond donors with greater electropositive character.

The Hill coefficient (η) for binding of fluoride to 3H(Phl^{Mes}) was also determined. The size of this parameter reflects the extent of cooperativity between supramolecular binding events.[47] The Hill coefficient (η) for binding of fluoride to 3H(Phl^{Mes}) was determined to be 5.0, which confirms that a large and positive allosteric interaction is at play for this system. Hill coefficients for the other phlorins studied range from 5.4 for 3H(Phl^{OMe}) to 8.6 for 3H(Phl^{F}). The trend along the series of phlorins tracks that of β_2 values, with the more electron deficient phlorin macrocycles displaying larger Hill coefficients.

The correlation between η and the electronic structure of the phlorin is illustrated by the plot in Figure 4. A linear relation exists between the oxidation potentials of the phlorins and the extent to which fluoride binding is cooperative. The less easily oxidized phlorins (i.e., those containing electron-withdrawing aryl groups at the 15-*meso*-position) display larger Hill coefficients for fluoride binding (Figure 4a). A similar relationship is evident upon comparing the log(β_2) values for 3H(Phl^{R})·2F$^-$ formation with the oxidation potentials of the parent phlorins (Figure 4b). This second correlation demonstrates that in addition to the level of cooperativity, the strength of the fluoride binding interaction can also be directly linked to phlorin electronic structure.

The extent to which binding of fluoride to the phlorin N–H residues perturbs the macrocycle's electronic properties is evident from UV–vis spectroscopy (vide supra). Formation of the fluoride bound adducts 3H(Phl^{R})·2F$^-$ also attenuates the porphyrinoids' redox properties (Table 2). As shown in Figure 5a, fluoride binding is manifest in large changes in the potentials at which 3H(Phl^{Mes})·2F$^-$ is oxidized, as judged by DPV experiments. For instance, the first oxidation potential ($E_{ox}(1)$) of this system shifts to less positive potentials by roughly 400 mV (Table 2). Similar results have been reported for fluoride binding to oxoporphyrinogen complexes in dichlorobenzene.[48] The second and third oxidation potentials also shift to less positive potentials by roughly 320 and 450 mV, respectively. Fluoride binding attenuates the potentials at which the other four phlorins are oxidized to a similar extent (Table S1), as observed variations in $E_{ox}(1)$ range from 210 to 540 mV (Table 2).

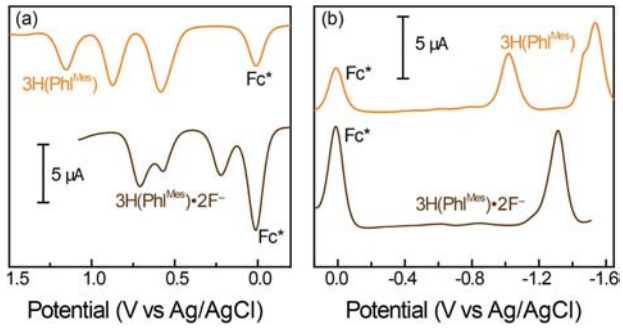

Figure 5. DPV traces recorded for 3H(Phl^{Mes}) (orange) and 3H(Phl^{Mes})·2F$^-$ (brown) in CH_2Cl_2 containing 0.1 M $TBAPF_6$ with an internal decamethylferrocene standard (FC*). DPV scans were recorded (a) to positive and (b) to negative potentials versus Ag/AgCl.

Association of 2 equiv of fluoride to 3H(Phl^{Mes}) also pushes the first reduction potential ($E_{red}(1)$) of the resultant 3H(Phl^{Mes})·2F$^-$ complex to more negative potentials (Figure 5b) by 280 mV. Similar behavior is observed for each of the other phlorins, where fluoride binding induces changes in $E_{red}(1)$ that range from 260 to 450 mV (Table 2).

■ SUMMARY AND CONCLUSIONS

The phlorin macrocycle has historically been an underdeveloped tetrapyrrole framework. Experiments have demonstrated that this porphyrinoid displays unique multielectron redox properties and a broad absorption profile that is well suited for solar harvesting applications.[25] In this work, we have roughly tripled the library of known 5,5-dimethylphlorin constructs by preparing a family of phlorins in which the aryl substituent at the 15-*meso*-position was systematically varied. All phlorins studied display a multielectron redox chemistry; each system can be oxidized three times at modest potentials and also displays two irreversible reduction waves. The electron-donating and withdrawing properties of the ancillary aryl substituent on the phlorin backbone attenuate the potentials of these redox events and provide a handle to tune the electrochemical properties of the porphyrinoid framework. Phlorin substitution also has a pronounced effect on the observed photophysics, as introduction of electron-releasing aryl groups on the periphery of the macrocycle is manifest in

dx.doi.org/10.1021/ja401391z | J. Am. Chem. Soc. 2013, 135, 6601–6607

larger emission quantum yields and longer fluorescence lifetimes.

All of the phlorins also display an intriguing supramolecular chemistry with fluoride anions. Each phlorin can bind 2 equiv of this halide in highly cooperative fashion. The strength and cooperative nature of fluoride binding to generate 3H-(Phl^R)·2F$^-$ correlate with the ability of the phlorin to stabilize the build-up of charge. Fluoride binding is manifest in dramatic changes to the phlorin electronic structure, as demonstrated by both UV−vis spectroscopy and electrochemistry experiments. Formation of 3H(Phl^R)·2F$^-$ is accompanied by increases in absorptivity and the appearance of strongly absorbing bands toward the near-IR region (750−900 nm). Fluoride binding also perturbs the ability of the phlorin to serve as an electron donor and/or acceptor, as each of the 3H(Phl^R)·2F$^-$ complexes is much more easily oxidized than the parent phlorins. Titration of phlorin with a source of fluoride represents a facile method to tune the ability of this porphyrinoid to absorb light and engage in redox chemistry. When coupled with the ability to modulate the phlorin's redox and photophysical properties via synthetic alteration of the macrocycle's periphery, this general framework provides a versatile platform with potential applications in the fields of photocatalysis, electrocatalysis, anion sensing, and solar-light capture. The modular synthesis of the phlorin framework, coupled with the flexibility offered by its supramolecular chemistry with fluoride, distinguishes this porphyrinoid from more commonly studied porphyrin and corrole macrocycles. As such, the phlorin is an intriguing candidate for incorporation into energy-storing schemes and colorimetric/electrochemical platforms for fluoride detection. Future efforts in our laboratory will focus on the use of phlorin frameworks for such endeavors.

■ ASSOCIATED CONTENT

Supporting Information

Synthetic procedures and spectroscopic data. This material is available free of charge via the Internet at http://pubs.acs.org.

■ AUTHOR INFORMATION

Corresponding Author

joelr@udel.edu

Notes

The authors declare no competing financial interest.

■ ACKNOWLEDGMENTS

We thank Sean Herron (University of Delaware) for assistance with UV−vis fluoride titration experiments. Research reported in this publication was supported by an Institutional Development Award (IDeA) from the National Institute of General Medical Sciences of the National Institutes of Health under Grant P20GM103541. J.R. also thanks the University of Delaware Research Foundation and the Donors of the American Chemical Society's Petroleum Research Fund for financial support. D.A.L. and Y.-Z.M. were sponsored by the Division of Chemical Sciences, Geosciences, and Biosciences, Office of Basic Energy Sciences, U.S. Department of Energy. NMR and other data were acquired at University of Delaware using instrumentation obtained with assistance from the NSF and NIH (Grants NSF-MIR 0421224, NSF-CRIF MU CHE-0840401 and CHE-0541775, and NIH P20 RR017716).

■ REFERENCES

(1) Milgrom, L. R. *The Colours of Life: An Introduction to the Chemistry of Porphyrins and Related Compounds*; Oxford University Press: New York, 1997.

(2) Gray, H. B.; Winkler, J. R. *Electron Transfer in Chemistry*; Wiley-VCH: Weinheim, Germany, 2001; Vol. *3.1.1*.

(3) Winkler, J. R.; Gray, H. B. *Chem. Rev.* **1992**, *92*, 369−379.

(4) Riggs, A. F. *Cur. Opin. Struct. Biol.* **1991**, *1*, 915−921.

(5) Sono, M.; Roach, M. P.; Coulter, E. D.; Dawson, J. H. *Chem. Rev.* **1996**, *96*, 2841−2888.

(6) Dunford, H. B. *Heme Peroxidases*; John Wiley: Chichester, U.K., 1999.

(7) Green, B. R.; Durnford, D. G. *Annu. Rev. Plant Physiol.* **1996**, *47*, 685−714.

(8) Ben-Shem, A.; Frolow, F.; Nelson, N. *Photosynth. Res.* **2004**, *81*, 239−250.

(9) Kerfeld, C. A.; Krogmann, D. W. *Annu. Rev. Plant Physiol.* **1998**, *49*, 397−425.

(10) Wasielewski, M. R. *Photochem. Photobiol.* **1988**, *47*, 923−929.

(11) Wasielewski, M. R. *Chem. Rev.* **1992**, *92*, 435−461.

(12) Hagfeldt, A.; Boschloo, G.; Sun, L.; Kloo, L.; Pettersson, H. *Chem. Rev.* **2010**, *110*, 6595−6663.

(13) Campbell, W. M.; Burrell, A. K.; Officer, D. L.; Jolley, K. W. *Coord. Chem. Rev.* **2004**, *248*, 1363−1379.

(14) Campbell, W. M.; Jolley, K. W.; Wagner, P.; Wagner, K.; Walsh, P. J.; Gordon, K. C.; Schmidt-Mende, L.; Nazeeruddin, M. K.; Wang, Q.; Gratzel, M.; Officer, D. L. *J. Phys. Chem. C* **2007**, *111*, 11760−11762.

(15) Wang, Q.; Campbell, W. M.; Bonfantani, E. E.; Jolley, K. W.; Officer, D. L.; Walsh, P. J.; Gordon, K.; Humphry-Baker, R.; Nazeeruddin, M. K.; Gratzel, M. *J. Phys. Chem. B* **2005**, *109*, 15397−15409.

(16) Papagiannakis, E.; Kennis, J. T. M.; van Stokkum, I. H. M.; Cogdell, R. J.; van Grondelle, R. *Proc. Natl. Acad. Sci. U.S.A.* **2002**, *99*, 6017−6022.

(17) Cerullo, G.; Polli, D.; Lanzani, G.; De Silvestri, S.; Hashimoto, H.; Cogdell, R. J. *Science* **2002**, *298*, 2395−2398.

(18) Frank, H. A.; Cogdell, R. J. *Photochem. Photobiol.* **1996**, *63*, 257−264.

(19) Yella, A.; Lee, H.-W.; Tsao, H. N.; Yi, C.; Chandiran, A. K.; Nazeeruddin, M. K.; Diau, E. W.-G.; Yeh, C.-Y.; Zakeeruddin, S. M.; Gratzel, M. *Science* **2011**, *334*, 629−634.

(20) Floriani, C.; Floriani-Moro, R. In *The Porphyrin Handbook*; Kadish, K. M., Smith, K. M., Guilard, R., Eds.; Academic Press: New York, 2000; Vol. *3*, pp 405−420.

(21) Korobkov, I.; Gambarotta, S.; Yap, G. P. A. *Angew. Chem., Int. Ed.* **2002**, *41*, 3433−3436.

(22) Harmjanz, M.; Gill, H. S.; Scott, M. J. *J. Am. Chem. Soc.* **2000**, *122*, 10476−10477.

(23) Harmjanz, M.; Scott, M. J. *Inorg. Chem.* **2000**, *39*, 5428−5429.

(24) Bachmann, J.; Hodgkiss, J. M.; Young, E. R.; Nocera, D. G. *Inorg. Chem.* **2007**, *46*, 607−609.

(25) Pistner, A. J.; Yap, G. P. A.; Rosenthal, J. *J. Phys. Chem. C* **2012**, *116*, 16918−16924.

(26) Krattinger, B.; Callot, H. J. *Tetrahedron Lett.* **1996**, *37*, 7669−7702.

(27) Hong, S.-J.; Ka, J.-W.; Won, D.-H.; Lee, C.-H. *Bull. Korean Chem. Soc.* **2003**, *24*, 661−663.

(28) O'Brien, A. Y.; McGann, J. P.; Geier, G. R. *J. Org. Chem.* **2007**, *72*, 4084−4092.

(29) Littler, B. J.; Miller, M. A.; Hung, C.-H.; Wagner, R. W.; O'Shea, D. F.; Boyle, P. D.; Lindsey, J. S. *J. Org. Chem.* **1999**, *64*, 1391−1396.

(30) Borbas, K. E.; Chandrashaker, V.; Muthiah, C.; Kee, H. L.; Holten, D.; Lindsey, J. S. *J. Org. Chem.* **2008**, *73*, 3145−3158.

(31) Kalyanasundaram, K. *Photochemistry of Polypyridine and Porphyrin Complexes*; Academic Press: San Diego, CA, 1991.

(32) Fonda, H. N.; Gilbert, J. V.; Cormier, R. A.; Sprague, J. R.; Kamioka, K.; Connolly, J. S. *J. Phys. Chem.* **1993**, *97*, 7024−7033.

(33) Grancho, J. C. P.; Pereira, M. M.; Miguel, M. d. G.; Gonsalves, A. M. R.; Burrows, H. D. *Photochem. Photobiol.* **2002**, *75*, 249−256.
(34) Moinet, C.; Simonneaux, G.; Autret, M.; Hindre, F.; Le Plouzennec, M. *Electrochim. Acta* **1993**, *38*, 325−328.
(35) Connelly, N. G.; Geiger, W. E. *Chem. Rev.* **1996**, *96*, 877−910.
(36) Woller, E. K.; DiMagno, S. G. *J. Org. Chem.* **1997**, *62*, 1588−1593.
(37) Gale, P. A.; Sessler, J. L.; Král, V.; Lynch, V. *J. Am. Chem. Soc.* **1996**, *118*, 5140−5141.
(38) Gale, P. A; Sessler, J. L; Král, V. *Chem. Commun.* **1998**, 1−8.
(39) Gale, P. A.; Anzenbacher, P., Jr.; Sessler, J. L. *Coord. Chem. Rev.* **2001**, *222*, 57−102.
(40) Sessler, J. L.; Cyr, M.; Furuta, H.; Král, V.; Mody, T.; Morishima, T.; Shionoya, M.; Weghorn, S. *Pure Appl. Chem.* **1993**, *65*, 393−398.
(41) Král, V.; Sessler, J. L.; Zimmerman, R. S.; Seidel, D.; Lynch, V.; Andrioletti, B. *Angew. Chem., Int. Ed.* **2000**, *39*, 1055−1058.
(42) Sessler, J. L.; Zimmerman, R. S.; Bucher, C.; Král, V.; Andrioletti, B. *Pure Appl. Chem.* **2001**, *73*, 1041−1057.
(43) Sessler, J. L.; Camiolo, S.; Gale, P. A. *Coord. Chem. Rev.* **2003**, *240*, 17−55.
(44) Ka, J.-W.; Lee, C.-H. *Tetrahedron Lett.* **2001**, *42*, 4527−4529.
(45) Shionoya, M.; Furuta, H.; Lynch, V.; Harriman, A.; Sessler, J. L. *J. Am. Chem. Soc.* **1992**, *114*, 5714−5722.
(46) Zhang, Y.; Li, M. X.; Lü, M. Y.; Yang, R. H.; Liu, F.; Li, K. A. *J. Phys. Chem. A* **2005**, *109*, 7442−7448.
(47) Weiss, J. N. *FASEB J.* **1997**, *11*, 835−841.
(48) Subbaiyan, N. K.; Hill, J. P.; Ariga, K.; Fukuzumi, S.; D'Souza, F. *Chem. Commun.* **2011**, *47*, 6003−6005.